

Phonon spectra and crystal structure of Zn and Cd using the resonant model-potential approach

J. C. Upadhyaya

Department of Physics, University of Maiduguri, Maiduguri PMB 1069, Nigeria

L. Dagens

Commissariat à l'Energie Atomique, B. P. No. 27, 94190 Villeneuve, St. Georges, France

(Received 8 June 1981)

In the present study, the resonant model potential (RMP) method derived for d -band metals is applied to the microscopic calculation of the phonon spectra and to the determination of the crystal structure of lowest energy of zinc and cadmium. The self-consistent RMP is of the form $v(E) = w(E) + A_d \mathcal{U} / (E - \mathcal{E})$, where $w(E)$ is a Heine-Abarenkov-type nonlocal model potential (including the self-consistent screening potential); the second term with $\mathcal{U} = \sum_m 4\pi\gamma(r)\gamma(r')Y_{2m}^*(\hat{r})Y_{2m}(\hat{r}')$ is a Heine-type resonant model potential which acts only on d states. The model parameters are determined so that the self-consistent Wigner-Seitz neutral pseudoatom potential is equivalent in the physical energy range to the Wigner-Seitz self-consistent potential calculated in the framework of the Hartree-Slater scheme. The model parameters are then used to calculate the phonon dispersion, bulk modulus, and the structural energy of Zn and Cd. The dispersion results and the bulk modulus are found in reasonably good agreement with the experimental data for both metals. Of course the calculation gives the stable hcp structure for the two metals, but the axial ratios are not predicted to be as high as the observed ones. In order to know the effect of the resonant part of the RMP, we performed calculations by neglecting the resonant part. This neglect results (a) in decreasing the value of the bulk modulus by about 20% for Zn and 15% for Cd, (b) in deducing the stable hcp structure at about the ideal axial ratio, and (c) in lowering the phonon frequencies in general by 25–30%. The strong near-resonance hybridization effect in the RMP has also been studied. Our calculations show this effect to be small on the bulk modulus and phonon frequencies of Zn.

I. INTRODUCTION

The two elements of the Periodic Table, Zn and Cd, are grouped together when the electronic structure and solid-state properties are studied, because (i) zinc and cadmium possess the highest axial ratio (c/a), 1.856 and 1.886, respectively, in the family of hexagonal close-packed (hcp) metals; (ii) both are divalent metals and are seen to be in the same column of the Period Table; (iii) both occupy the position of bridge elements between the simple and transition metals; (iv) the two metals possess a similar s - d interaction, and (v) in both of the metals, the filled d bands lie below the Fermi energy. Therefore, we have chosen these elements to study the microscopic interactions in the crystal state in order to derive some important electronic properties. In accordance with the idea of scattering resonances in d band metals,^{1–4} a resonant model po-

tential (RMP) was previously developed by one of us.^{5,6} Dagens^{6–8} and Upadhyaya and Dagens^{9,10} successfully applied this model potential method in the explanation of many electronic properties of noble metals. Since characteristics (iii)–(v) of Zn and Cd, discussed above, are similar to those of noble metals, the extension of the RMP method for the study of the electronic structure and properties of Zn and Cd seemed appealing to us.

In order to study the lattice dynamics of Zn and Cd, earlier workers^{11–14} applied the Heine-Abarenkov-Animalu (HAA) and Shaw's optimized model potential (OMP) methods for simple metals. When the work of Brovman *et al.*¹¹ with the HAA method and that of Gilat *et al.*¹² with the OMP method are reviewed, it is found that both procedures give imaginary phonon frequencies at some points of the Brillouin zone. Recent works of Kulshrestha and Upadhyaya¹³ and Kumar and

Upadhyaya¹⁴ are successful attempts in explaining the phonon spectra of zinc by improving the HAA and transition-metal model potential (TMMP) methods in the full scheme of Eschrig and Wonn.¹⁵ The scheme of Kulshrestha and Upadhyaya¹³ is not satisfactory because it uses two adjustable parameters. Of course, in the work of Kumar and Upadhyaya,¹⁴ the nonlocal parameters are derived from the model potential and basic data but with the approximation that the nonlocal parameter a_q (and hence b_q) is determined by averaging its value for the scattering vectors lying on the Fermi surface.

In the case of Zn and Cd, one would like to ask: What is the role of d electrons in the lattice dynamics and crystal structure of these metals? Moriarty¹⁶ was the first to apply the generalized pseudopotential theory of Harrison¹⁷ to calculate the form factor of Zn with and without hybridization. The computed results show that the effect of the hybridization on the form factor is not serious. Later, he refined the theory by introducing a zero-order pseudoatom approach¹⁸ in which the core and d states and their eigenvalues are precisely defined and also in which an accurate evaluation of the matrix elements of both the pseudopotential w_0 and the hybridization potential Δ is possible. In the case of Zn and Cd the effect of hybridization on the form factor is again found not to be substantial but is seen to be contributory in the calculation of other electronic properties, leading Moriarty to conclude that these metals are to be treated as d -band metals. In further work, Moriarty¹⁹ reformulated the generalized pseudopotential theory from the self-consistent field equations of Kohn and Sham²⁰ in conjunction with the zero-order pseudoatom approach. In this work the attention is given to the structure dependence of Δ , neglected in previous work. The structure-dependent parts of Δ lead to a modified energy wave-number characteristic and a d -state overlap potential. One interesting result of Δ (structure) inclusion is that the predicted stable structure of Zn and Cd is found to be hcp with the axial ratios very near to the observed values. Panitz *et al.*²¹ applied the generalized Harrison's pseudopotential formalism with a Lindgren-type approximation for the conduction-band—core-electron exchange to compute the dispersion relations for Zn along the ΓM direction. They found that the results of this calculation differ slightly with those obtained by treating Zn as simple metal. In a later work Cutler *et al.*²² gave an exact treatment for the

orthogonalization hole in Harrison's pseudopotential theory²³ and computed the phonon dispersion curves along ΓKM direction for Zn by using the Harrison's simple-metal and generalized pseudopotential theories with the same approximation for conduction-band—core-electron exchange, as used by Panitz *et al.*²¹ The difference seen in the results of the two calculations is not great, but it is notable. It is noted that in the calculations of Panitz *et al.*²¹ and Cutler *et al.*²² real phonon frequencies for all the dispersion branches for Zn are obtained when the Lindgren-type approximation for the conduction-band—core-electron exchange, suitable for d -band metals, is used in the simple as well as in the generalized pseudopotential theories of Harrison. The Kohn-Sham approximation,²⁰ suitable for nearly-free-electron metals, gives imaginary phonon frequencies for many branches for Zn. Thus one may conclude from these works that the effect of d electrons must be taken into account in the study of the electronic properties of Zn. In the present work, effort has been made to analyze the effect of the s - d interaction on the lattice dynamics and crystal structure of Zn and Cd in the resonant model potential theory.

In order to make the work self-contained, the essentials of the resonant model potential theory are first discussed briefly in Sec. II. The hybridization effect is considered in detail, especially pointing out that no overlap contribution occurs in the present approach. Next, the procedure for the determination of model parameters is discussed briefly. The model parameters are then applied in the calculation of form factor, energy wave-number characteristic, phonon frequencies, bulk modulus, and structural energies of Zn and Cd. Numerical results, a discussion, and some conclusions are presented in Sec. III.

II. THEORY

A. Metal energy

First, the theory of the resonant model potential⁵⁻⁸ (RMP) is briefly presented. The metal potential is replaced by an equivalent self-consistent nonlocal and energy-dependent RMP $V(E)$. Using a linear screening approximation, $V(E)$ is obtained (up to an unimportant constant) by a sum of neutral pseudoatom potentials $\sum_{\text{ions}} v(E)$. Its plane-wave matrix element between $|\vec{k}\rangle$ and $|\vec{k} + \vec{q}\rangle$ has the standard form^{17,24} $NS(\vec{q})v(\vec{q}, \vec{k}, E)$ with

$$v(\vec{q}, \vec{k}, E) = w(\vec{q}, \vec{k}, E) + \frac{A_d}{E - \mathcal{E}} \mathcal{U}(\vec{q}, \vec{k}), \quad (1)$$

and $NS(\vec{q}) = \sum_a \exp i \vec{q} \cdot \vec{R}_a$. The matrix elements are normalized in the unit cell. The RMP (1) includes a regular Heine-Abarenkov-type part which can be written in \vec{r} space as

$$\begin{aligned} w &= w_{\text{loc}} + w_{\text{nonloc}} \\ &= -\frac{Ze^2}{r} + \gamma(R_m - r) \left[\frac{Ze^2}{r} - \frac{Ze^2}{R_m} \right] \\ &\quad + w_{\text{sc}}(r) + \sum_l w_l(r) \mathcal{P}_l, \end{aligned} \quad (2)$$

where Z is the charge of the model ion, being equal to the sp valence charge ($Z=2$ for Zn and Cd) and $w_{\text{sc}}(r)$ is the screening potential. The operator \mathcal{P}_l projects on the l angular momentum states, and

$$w_l(r) = \left[\frac{Ze^2}{R_m} - A_l(E) \right] \gamma(R_m - r), \quad (3)$$

so that $w_l(r)$ vanishes outside the model radius R_m . Only A_0 and A_1 are nonzero in the present work. The d potential is modeled through the resonant part and the $l \geq 3$ terms are neglected.

The singular contribution in Eq. (1) is the resonant part of the RMP. It acts only on d states and is separable in each m channel.⁵ The expression for \mathcal{U} is

$$\begin{aligned} \mathcal{U}(\vec{q}, \vec{k}) &= 4\pi \gamma(\vec{k} + \vec{q}) \gamma(k) \\ &\quad \times \sum_m Y_{2m}(\hat{k}') Y_{2m}^*(\hat{k}), \end{aligned} \quad (4)$$

where $\gamma(k)$ is the j_2 Bessel transform of a function which behaves as r^2 when $r \rightarrow 0$ and which vanishes for $r > R_m$. The form

$$\gamma(k) = j_2(kR_m) / (1 - k^2 R_m^2 / x_0^2) \quad (5)$$

is used here.⁶⁻⁸ x_0 is the first zero of $j_2(x)$.

The parameter A_d in (1) controls the strength of the resonance and \mathcal{E} its position. But \mathcal{E} is quite different from the physical resonance energy E_d and must be renormalized before doing the perturbation expansion described below.^{6,7} The isolated RMP scattering matrix is easily calculated as

$$\begin{aligned} t_{\text{res}}(E) &= A_d \left[E - \mathcal{E} - \frac{\Omega_d A_d}{(2\pi)^3} \right. \\ &\quad \left. \times \int d\vec{k} \frac{\gamma(k)^2}{E + i\eta - \hbar^2 k^2 / 2m} \right]^{-1}. \end{aligned} \quad (6)$$

The denominator is of the form $E - \mathcal{E} - B(E) + i\Gamma(E)$. $\Gamma(E)$ is the virtual bound-state half-width²⁵ and is small for the 3d transitional-metal series. The physical resonance occurs at

$$E_d = \mathcal{E} + B(E_d). \quad (7)$$

The quantity $B(E)$ turns out to be large. A resummation of the A_d expansion [such as (6)] is necessary to get meaningful results. This can be done in a consistent way as discussed in the work of Dagens.⁶ In the procedure, the RMP is replaced by

$$\lambda v_{\text{res}}(\lambda) = \frac{\lambda A_d}{E - \tilde{\mathcal{E}}(E) + \lambda B(E)}, \quad (8)$$

where

$$\tilde{\mathcal{E}}(E) = \mathcal{E} + B(E) - \Delta E_F. \quad (9)$$

The Fermi-level first-order change $E_F - E_{F0} = \Delta E_F$ has been subtracted so that $\tilde{\mathcal{E}}(E_d) - E_{F0}$ approximates $E_d - E_F$. A physical quantity is then systematically expanded up to a given order of λ .

The result is thus given by a series involving the renormalized potential $A_d \mathcal{U} / (E - \tilde{\mathcal{E}})$ (with $\tilde{\mathcal{E}}$ of the order of E_d). The whole series calculated for $\lambda=1$ gives the exact result since $v_{\text{res}}(\lambda=1) = A_d \mathcal{U} / (E - \mathcal{E})$. In the present work we are interested in the lowest order $O(\lambda^2)$ structure-dependent energy, which can be obtained by using the renormalized potential in (1) in place of the true one.

The total energy E_{tot} can then be expanded in terms of λ provided that $|E - E_d|$ is much larger than Γ (Dagens⁷). This corresponds to a full d band when $E_d \ll E_F$ (Zn, Cd) and empty d band when $E_d \gg E_F$ (Ca, for instance). The total energy is

$$E_{\text{tot}} = E_b - E_{ee} + E_{ii}, \quad (10)$$

where E_b denotes the band energy $\sum_{\text{occ}} E_k$; E_{ee} is the electron-interaction energy and is subtracted in order to correct for double counting. The last term is the ion-ion interaction energy. The band energy is given by Eq. (21) of Ref. 7:

$$\begin{aligned} E_b &= NZ_d E_d + NZ E_{\text{EG}} \\ &\quad - \frac{1}{2\pi i} \int_c dz \text{Tr} \ln \left[1 - \frac{1}{H_0 - z} V(z) \right], \end{aligned}$$

where Z_d is the number of d electrons ($=10$ when $E_d \ll E_F$) and N the number of ions. E_{EG} is the homogeneous electron gas energy per electron and

is irrelevant in the present problem. Only the last term includes structure-dependent terms and is considered here. The Tr is a trace over all of the electronic states. The contour c encloses the semiaxis $E < E_F$ counterclockwise. It can be

$$E_{b \text{ str}} = \frac{1}{2\pi i} \frac{1}{2} \int_{c_0} dz \text{Tr} \frac{1}{z - H_0} V(z) \frac{1}{z - H_0} V(z) = \sum_{\vec{q}} |S(\vec{q})|^2 \frac{1}{2\pi i} \int_{c_0} dz \sum_{\vec{k}\sigma} \frac{[V(\vec{q}, \vec{k}, z)]^2}{(z - E_k^0)(z - E_{\vec{k} + \vec{q}}^0)}.$$

The contour integration is easily done and the result is

$$E_{b \text{ str}} = \frac{N}{2} \sum_{\vec{q}} |S(\vec{q})|^2 [\phi_{ss}(q) + \phi_{sd}(q) + \phi_{dd}(q)], \quad (11)$$

with

$$\phi_{ss}(q) = \frac{4\Omega_a}{(2\pi)^3} \int d\vec{k} \frac{f_{\vec{k}}}{E_{\vec{k}} - E_{\vec{k}'}} |w(\vec{k}, \vec{k}'; E_{\vec{k}'})|^2, \quad (12a)$$

$$\phi_{sd}(q) = \frac{8\Omega_a}{(2\pi)^3} \int d\vec{k} \frac{f_{\vec{k}} - f_d}{E_{\vec{k}} - E_{\vec{k}'}} w(\vec{k}, \vec{k}'; E_k) \times \tilde{V}_{\text{res}}(\vec{k}, \vec{k}'; E_k), \quad (12b)$$

$$\phi_{dd}(q) = \frac{4\Omega_a}{(2\pi)^3} \int d\vec{k} \frac{f_{\vec{k}} - f_d}{E_{\vec{k}} - E_{\vec{k}'}} \times |\tilde{V}_{\text{res}}(\vec{k}, \vec{k}'; E_k)|^2, \quad (12c)$$

where f_d is the d -state occupation number ($f_d = 1$ when $E_d \ll E_F$). The first term ϕ_{ss} is as in the simple-metal theory.²⁴ ϕ_{sd} represents the contribution associated to electronic transition between a resonant or hybridized state d at site i and a non-resonant state s at another ionic site j . ϕ_{dd} is associated to the scattering between two resonant states di and dj . Both terms involve the hybridization coefficient $\gamma(k)$ and are thus hybridization contributions. Other hybridization contributions [i.e., terms involving $\gamma(k)$] are implicit in ϕ_{ss} since w includes a screening part induced by the resonant part of the potential (see below).

One notes that no overlap contribution appears in the present theory. The lack of overlap contribution can be ascribed to the nonoverlap requirement for the model spheres^{5,6} which allows a simple and accurate description of the strong d potential in terms of a resonant $l=2$ phase shift (or equivalently in terms of an energy-dependent loga-

chosen so that $|E_d - z|$ is never smaller than $|E_d - E_F|$. $V(z)$ is then small and the logarithm can be expanded in terms of λ and $w_0(z)$. The lowest-order structure-dependent term is given by

rithmic derivative at a radius not greater than the muffin-tin radius R_{MT}). Similarly, nonoverlap contributions are to be added when the energy is calculated from the Korringa-Kohn-Rostoker (KRR) method, where plane waves only are used to describe the wave function outside the muffin-tin spheres.

The overlap energy E_{Ol} arises in the generalized pseudopotential theory¹⁶ (GPT) when a set of overlapping d atomiclike or localized wave functions φ_d are used to describe the resonant state. On the other hand, Moriarty¹⁶ has shown that the choice of φ_d is quite flexible and that E_{Ol} depends on this choice. Moreover, the choice of nonoverlapping φ_d is consistent with the general theory; this choice (which may prove to be inconvenient in practice) leads to an exactly equivalent pseudo-Hamiltonian with no overlap contribution, as in the RMP theory.

When a GPT gives a nonvanishing overlap energy, where is its numerical counterpart in the RMP theory? The overlap contribution involves transition matrix elements between two zero-order resonant states¹⁶ and is thus a first contribution associated to the scattering between two resonant states (a second contribution arises from the hybridization potential); its numerical counterpart should thus be included in ϕ_{dd} .

As stated above, $w(\vec{q}, \vec{k})$ includes the self-consistent screening potential due to the screening density $n_{sc}(q)$ which is made of two parts: the model density $n_{ps}(q)$ to be calculated from the model wave functions and the depletion charge density $n_{dpl}(q)$ which corrects for the difference between the true and model wave function.²⁴ The metal model density $S(\vec{q})n_{ps}(q)$ can be calculated⁶ from (11) using the perturbation formula

$$\delta E_{b \text{ str}} = NS(\vec{q})n_{ps}(q)\delta V(\vec{q}).$$

This together with (2) leads to a linear self-consistency equation for n_{ps} and the resulting linear screening charge turns out to be

$$n_{sc}(q) = n_{ps}(q) + n_{dpl}(q)$$

$$= \frac{1}{\tilde{\epsilon}(q)} \left[n_{dpl}(q) + \frac{2}{\Omega} \sum_{\vec{k}} \frac{\Omega_a w_0(\vec{q}, \vec{k}, E_{\vec{k}})}{E_k - E_{\vec{k} + \vec{q}}} + \frac{2}{\Omega} \sum_{\vec{k}} \frac{(f_k - f_a) \Omega_a \mathcal{U}(\vec{q}, \vec{k})}{(E_k - E_{\vec{k} + \vec{q}})(E_k - \tilde{\mathcal{E}})} \right], \quad (13)$$

with

$$\tilde{\epsilon}(q) = 1 + I(q) \frac{mk_F}{\pi^2 \hbar^2} \left[\frac{1}{2} + \frac{1-x^2}{4x} \ln \left| \frac{1+x}{1-x} \right| \right], \quad (14)$$

where $x = q/2k_F$. $I(q) = 4\pi e^2/q^2 + x(q)$, where $x(q)$ is the effective exchange and correlation interaction. The two first terms in (13) are present in the simple-metal model potential theory. The last term is the resonant part contribution. The depletion density is of the form $Z_{dpl} \nu(q)$ [$\nu(0) = 1$] where $\nu(q)$ is the Fourier transform of $\gamma(R_m - r)/\Omega_m$ (Ω_m is the model volume). The depletion Z_{dpl} is determined so that $n_{sc}(0) = Z$ [this means that the ion is perfectly screened by $n_{sc}(q)$].

We now give the expression of the total energy or rather of its structure-dependent contribution. The last two terms in (10) can be written as (Dagens⁷)

$$NU_{Ew}(Z_{eff}) - \frac{N}{\Omega_a} \sum_{\vec{q}} |S(\vec{q})|^2 I(q) [n_{ps}(q)^2 - n_{dpl}(q)^2], \quad (15)$$

where $U_{Ew}(Z_{eff})$ is the Ewald electrostatic energy calculated for the effective charge Z_{eff} defined by

$$Z_{eff}^2 = n_{ps}(0)^2 - n_{dpl}(0)^2 = (Z - Z_{dpl})^2 - Z_{dpl}^2. \quad (16)$$

Adding (15) to $E_{b\text{ str}}$, the final expression for the structural energy is found to be

$$E_{str} = N \frac{1}{2} \sum_{\vec{q}} |S(\vec{q})|^2 F(q) + NU_{Ew}(Z_{eff}),$$

with

$$F(q) = -\frac{4\pi e^2 Z_{eff}^2}{\Omega_a q^2} F_N(q) = \phi_{ss}(q) + \phi_{sd}(q) + \phi_{dd}(q) + \frac{I(q)}{\Omega_a} [n_{dpl}(q)^2 - n_{ps}(q)^2], \quad (17)$$

where $F_N(q)$ is the normalized energy wave number characteristic.

Only $F(q)$ and Z_{eff} are required for the phonon problem. The numerical calculation of $F(q)$ is as described in Ref. 7. $n_{ps}(q)$ is first calculated from (13); ϕ_{ss} and ϕ_{sd} [which both require $w = w_{ion} + I(q)n_{sc}$] and ϕ_{dd} are then calculated. The \vec{k} integrations in (12) and (13) are done exactly as described by Moriarty.¹⁶ Z_{dpl} is found from the perfect screening relation $Z_{dpl} = Z - n_{ps}(0)$ and Z_{eff} from (16).

B. The potential parameters

The RMP parameters are determined for Zn and Cd as for the noble metals.⁸ They are calculated from first principles by requiring that the screened metal RMP is equivalent to the true Hartree-Fock-Slater (HFS) self-consistent potential. This is done using a Wigner-Seitz spherical approximation consistently for the HFS potential and for the model potential.

The first step is the calculation of the self-consistent HFS potential according to

$$\mathcal{V}_{WS}(r) = \left[-\frac{Z_N e^2}{r} + \frac{e^2}{r} \rho(r) + \mu_{KS}(\rho) - C \right] \gamma(R_a - r), \quad (18)$$

where

$$\rho(r) = [|\Psi_{4s}(r)|^2 + 10 |\Psi_{3d}(r)|^2 r^2 + \rho_{core}(r)] \gamma(R_a - r). \quad (19)$$

R_a is the mean atomic radius, ρ_{core} the ionic core density, Ψ_{4s} and Ψ_{3d} the radial Wigner-Seitz wave function (both satisfying the even l Wigner-Seitz boundary condition $\partial\Psi_l/\partial r = 0$ at $r = R_a$), and μ_{KS} is Kohn-Sham effective exchange potential

$$\mu_{KS}(\rho) = -e^2(3\rho/\pi)^{1/3}. \quad (20)$$

The constant C in (18) is chosen so that the Friedel sum $\sum_l (2/\pi) \eta_l(E_{F0})$ vanishes. This choice is convenient because the same property holds for the equivalent model potential so that $E_F = E_{F0}$ to second order.

The next step is the calculation of the local potential of the WS neutral pseudoatom. The screening density is written as

$$\rho_{sc}(r) = \frac{Z}{\Omega_a} \gamma(R_a - r) + \frac{Z_{dpl}}{\Omega_m} \gamma(R_a - r) + 10 \frac{1}{r^2} \varphi_d(r)^2. \quad (21)$$

The first two terms are, respectively, the zero-order sp density and the depletion charge density (Ω_m is the model sphere volume $4\pi R_m^3/3$). φ_d is the model radial wave function normalized so that $\varphi_d(R_m) = \Psi_d(R_m)$. Z_{dpl} is determined so that $\int \rho_{\text{sc}}(r)d\vec{r} = Z$. The function $\phi_d(\vec{r}) = (1/r)\varphi_d Y_{20}$ must satisfy the Schrödinger equation

$$-\frac{\hbar^2}{2m}\Delta\phi_d + \mathcal{A}\mathcal{U}\phi_d + (w_{\text{loc}} - C')\phi_d = E_d\phi_d, \quad (22)$$

with the boundary condition $\partial\varphi_d/\partial r = 0$ at $r = R_a$. E_d is the $3d$ state energy determined above using the potential $\mathcal{V}_{\text{WS}}(\vec{r})$. w_{loc} is $-Ze^2/r + \mathcal{V}_e(\rho_{\text{sc}})$ and the constant C is chosen so that $\mathcal{V}_{\text{WS}} - C$ and $w_{\text{loc}} - C'$ are equal at $r = R_a$ (the potentials are then nearly equal outside the model region, an essential requirement in model potential theory²⁴). $\mathcal{A}\mathcal{U}$ is the resonant potential for $E = E_d$. The calculation is iterative ($\mathcal{A} \rightarrow \varphi_d \rightarrow Z_{\text{dpl}} \rightarrow w_{\text{loc}} \rightarrow \mathcal{A}$) and its result is the self-consistent WS local potential $w_{\text{loc}}(r)$.

The last step is to determine A_0 , A_1 , and \mathcal{A} [the RMP is written as $\mathcal{A}(E)\mathcal{U}$] so that model and true wave functions' logarithmic derivatives agree at $r = R_a$. This is done successively for $l=0, 1$, and 2 for nine values of E ($E = 0.2nE_{F0}$, $n=0, 1, \dots, 8$). The model radius R_m has been chosen so that the $l=0$ part is optimized²⁴ for $E = E_{F0}$. The results obtained for Zn and Cd are similar to those obtained for the noble metals⁸: $A_0(E)$, $A_1(E)$, and $\mathcal{A}(E)^{-1}$ turn out to be nearly linear functions of E . $\mathcal{A}(E)^{-1}$ is then fitted as $(E - \xi)/A_d$ in the vicinity of E_{F0} (ξ is of course the nonrenormalized resonant energy parameter; one notes that \mathcal{A} is

regular for $E = E_d$ since $\xi > E_d$).

The RMP parameters calculated for Zn and Cd as described above are displayed in Table I. The two A_l are determined by $A_l(E_F)$ and dA_l/dE_F . The renormalized $\tilde{\xi}(E_F)$ are also given. $\tilde{\xi}(E_d)$ is found to be in good agreement with E_d (the WS $3d$ state energy).

C. Calculation of phonon frequencies

In case of an hcp metal, the phonon frequencies ν corresponding to a wave vector \vec{q} ($|\vec{q}| = 2\pi/\lambda$) are determined by solving the secular equation

$$|\underline{D}(\vec{q}) - \omega^2 \underline{I}| = 0, \quad (23)$$

where $\underline{D}(\vec{q})$ is the dynamical matrix of order (6×6) because hcp structure consists of two atoms per unit cell; $\omega (= 2\pi\nu)$ are the circular photon frequencies and \underline{I} the unit matrix.

The dynamical matrix elements $D_{\alpha\beta}(\vec{q}, \kappa\kappa')$ are assumed to be composed of ion-ion electrostatic and band-structure parts, i.e.,

$$D_{\alpha\beta}(\vec{q}, \kappa\kappa') = D_{\alpha\beta}^i(\vec{q}, \kappa\kappa') + D_{\alpha\beta}^{bs}(\vec{q}, \kappa\kappa'), \quad (24)$$

where $\alpha, \beta = x, y, z$ and $\kappa, \kappa' = 1, 2$.

The electrostatic contribution to the dynamical matrix can be calculated with the help of Ewald's Θ -function transformation and the relevant expression for the computation can be had from the work of Reissland and Ese²⁶ but with the effective charge Z_{eff} . The band-structure part of the dynamical matrix is calculated in the resonant model potential theory and the relevant expressions for its evaluation are the following:

$$D_{\alpha\beta}^{bs}(\vec{q}, \kappa\kappa') = \omega_0^2 \sum_{\vec{h}} \frac{(\vec{q} + \vec{h})_{\alpha} (\vec{q} + \vec{h})_{\beta}}{|\vec{q} + \vec{h}|^2} F_N(|\vec{q} + \vec{h}|) \exp(-i\vec{h} \cdot \vec{r}_{\kappa\kappa'}),$$

$$D_{\alpha\beta}^{bs}(\vec{q}, \kappa\kappa') = \omega_0^2 \sum_{\vec{h}} \left[\frac{(\vec{q} + \vec{h})_{\alpha} (\vec{q} + \vec{h})_{\beta}}{|\vec{q} + \vec{h}|^2} F_N(|\vec{q} + \vec{h}|) - \frac{\vec{h}_{\alpha} \vec{h}_{\beta}}{|\vec{h}|^2} F_N(|\vec{h}|) G(\kappa) \right], \quad (25)$$

where $\omega_0^2 = 4\pi(Ze)^2/M\Omega$, M being the ionic mass and Ω the unit-cell volume (i.e., $\Omega = 2\Omega_a$ and $\omega_0^2 = \omega_p^2/2$, ω_p being the plasma frequency). The function

$$G(\kappa) = \sum_{\kappa'} \cos(\vec{h} \cdot \vec{r}_{\kappa\kappa'})$$

and \vec{h} are the reciprocal-lattice vectors. The function $F_N(q)$ is the normalized energy wave number characteristic, as defined earlier.

Finally, if the band-structure part is added to the Coulombic part, one can calculate the phonon frequencies corresponding to any wave vector \vec{q} . In the present work, we have calculated the phonon frequencies along three high-symmetry directions, namely ΓA , ΓM , and ΓKM , in which the secular equation assumes a simple form. The relevant expressions are given in the paper of Upadhyaya and Animalu.²⁷

III. NUMERICAL RESULTS AND DISCUSSION

The model parameters, given in Table I, are used to compute the form factor and energy wave number characteristic of Zn and Cd. We have given the plot of form factor for Zn in Fig. 1 by solid lines. The normalized energy wave number characteristic $F_N(q)$ has been calculated by using Eq. (17) and the results of calculation are presented in Table II. Next, the expressions (25) are used to compute the band-structure part of the dynamical matrix and the expressions of Reissland and Ese²⁶ are used to calculate the Coulombic contributions. The Coulomb part is then properly added to the band-structure part and the phonon frequencies are calculated for various reduced \vec{q} values along ΓA , ΓM , and ΓKM directions. Next, the phonon dispersion curves are plotted for Zn and Cd which have been shown in Figs. 2 and 3 with the experimental points of Almqvist and Stedman²⁸ and Toussaint and Champier,²⁹ respectively. We find that in both cases our numerical results for phonon dispersion are in good agreement with the experimental data. In the case of Zn, if we compare our results to those of Kumar and Upadhyaya¹⁴ and also to those of Panitz *et al.*²¹ and Cutler *et al.*²² by using the Harrison's generalized pseudopotential approach, we see that our dispersion curves are in better agreement with the neutron data than those of Kumar and Upadhyaya¹⁴ and have the same order of agreement as those of Panitz *et al.*²¹ and Cutler *et al.*²² Further, in case of Cd, our first-principle calculations are in close agreement with the experimental data when compared to those of Kulshrestha and Upadhyaya¹³ based on two adjustable parameters of the Eschrig and Wonn theory.¹⁵

In order to know the effect of the resonant part of the RMP, we have calculated the bulk modulus

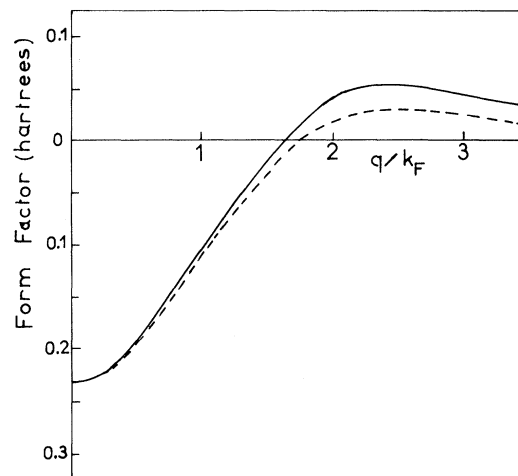


FIG. 1. Form factor of Zn: solid curves correspond to the resonant model potential (RMP) and the dotted ones to the potential with $A_d=0$.

and the structural energies corresponding to the bcc, fcc, and hcp phases with and without the resonant part of the potential for Zn and Cd. Phonon frequencies for Zn have also been computed without including the resonant part of the model potential. The calculation of bulk modulus is done as described earlier.⁷ The method of long wave is used. The bulk modulus is given by the sum of an electrostatic contribution and a band-structure contribution which involves the band-structure characteristic $F(q)$ given above. The formulas are standard and given, for instance, by Wallace.³⁰ The hcp energy has been calculated for various c/a ratios ranging from 1.6 to 2.0 and a minimum has been found in every case. The calculation for the potential without the resonant part is done using the same computer code and the same input data

TABLE I. Model parameters for zinc and cadmium. k_F is the zero-order Fermi momentum $(3\pi^2\Omega_a)^{-1}$. a and c are the lattice parameters. k_F , a , and c are in atomic units and all energies in hartrees.

	Zn	Cd		Zn	Cd
a	5.0341	5.613	$A_0(E_F)$	0.467	0.448
c	9.345	10.60	$\partial A_0/\partial E_F$	-0.23	-0.27
k_F	0.8342	0.7423	$A_1(E_F)$	0.617	0.545
R_m	2.14	2.23	$\partial A_1/\partial E_F$	-0.01	-0.04
A_d	0.0118	0.0147	Z_{eff}	2.314	2.523
\mathcal{E}	0.092	0.260			
$\tilde{\mathcal{E}}(E_F)$	0.006	-0.10			

TABLE II. The renormalized energy wave number characteristic $F_N(q)$.

q/k_F	Zn	Cd	q/k_F	Zn	Cd
0.0	1.000 00	1.000 00	2.6	0.002 93	-0.003 97
0.1	0.988 05	0.988 89	2.7	0.002 58	-0.002 99
0.2	0.952 93	0.956 19	2.8	0.001 97	-0.002 39
0.3	0.896 88	0.903 79	2.9	0.001 24	-0.002 14
0.4	0.823 58	0.834 84	3.0	0.000 27	-0.002 37
0.5	0.737 37	0.753 10	3.1	-0.000 67	-0.002 88
0.6	0.643 16	0.662 89	3.2	-0.001 73	-0.003 79
0.7	0.545 83	0.568 66	3.3	-0.002 73	-0.004 91
0.8	0.449 92	0.474 62	3.4	-0.003 69	-0.006 23
0.9	0.359 30	0.384 51	3.5	-0.004 54	-0.007 63
1.0	0.276 98	0.301 36	4.0	-0.006 41	-0.013 14
1.1	0.205 03	0.227 39	4.5	-0.008 86	-0.012 82
1.2	0.144 62	0.163 98	5.0	-0.002 84	-0.009 00
1.3	0.096 07	0.111 72	5.5	-0.001 89	-0.005 90
1.4	0.059 02	0.070 48	6.0	-0.001 53	-0.004 57
1.5	0.032 58	0.039 60	6.5	-0.001 04	-0.003 48
1.6	0.015 48	0.017 98	7.0	-0.000 57	-0.002 25
1.7	0.006 18	0.004 26	7.5	-0.000 28	-0.001 19
1.8	0.002 88	-0.003 14	8.0	-0.000 15	-0.000 68
1.9	0.003 39	-0.006 10	8.5	-0.000 04	-0.000 24
2.0	0.003 78	-0.000 749	9.0	-0.000 02	-0.000 20
2.1	0.002 61	-0.008 74	9.5	-0.000 00	-0.000 08
2.2	0.002 63	-0.008 56	10.0		-0.000 04
2.3	0.002 83	-0.007 71			
2.4	0.003 02	-0.006 49			
2.5	0.003 08	-0.005 18			

as the RMP case except for the hybridization strength parameters A_d , which would be set equal to zero. The use of the $A_d=0$ potential amounts to neglect of the hybridization potential, and the change with respect to the full RMP case is twofold: first, the ϕ_{sd} and ϕ_{dd} terms are absent and

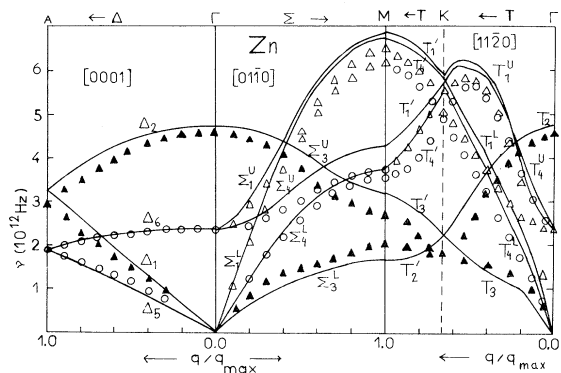


FIG. 2. Phonon dispersion in Zn: solid curves represent the results of present calculation and \blacktriangle , \triangle , \circ are the experimental points of Almqvist and Stedman (Ref. 28).

second, the screening induced by the hybridization is consistently omitted. We have plotted the corresponding form factor in Fig. 1 by dotted lines.

The numerical results for the structural energies and bulk modulus are given in Table III. The experimentally observed hcp structure is favored over

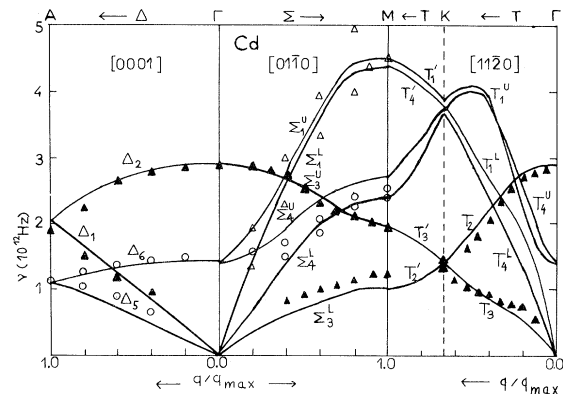


FIG. 3. Phonon dispersion in Cd: solid curves represent the results of present calculation and \blacktriangle , \triangle , \circ are the experimental points of Toussaint and Champier (Ref. 29).

TABLE III. Bulk modulus B (in units of 10^{12} dy/cm²) and structural energies calculated from the full RMP and from the potential without the resonant part ($A_d=0$). The energy difference (in units of 10^{-4} hartrees) $U_{\text{bcc}} - U_{\text{hcp}}$, . . . , are given with respect to the hcp structure for $(c/a)_{\text{min}}$ giving the lowest hcp energy.

	Zn			Cd		
	RMP	$A_d=0$	observed	RMP	$A_d=0$	observed
$(c/a)_{\text{min}}$	1.705	1.641	1.86	1.720	1.642	1.89
$U_{\text{bcc}} - U_{\text{hcp}}$	19.5	14.1		17.8	13.2	
$U_{\text{fcc}} - U_{\text{hcp}}$	9.2	7.0		7.5	5.3	
B	0.5910	0.472	0.6101 ^a	0.3905	0.3180	0.477 ^a

^aRoom-temperature isothermal bulk modulus (Ref. 31).

the bcc and fcc structures when both potentials are used. The RMP values of $(c/a)_{\text{min}}$ are greater than the ideal values but are lower than the observed ones. It is also observed that the neglect of the resonance term ($A_d=0$) leads to nearly the ideal c/a ratio and to smaller differences in energy. The ionic nonlocal d potential, which is used in the present work [Eq. (1)] as a resonant potential, has thus a significant effect on the Zn and Cd structural energies.

For the two metals under consideration, the bulk modulus has been also calculated (Table III). Good agreement with the experiment for Zn and a moderate agreement for Cd is obtained when the full RMP is used. The neglect of the resonant part leads to significantly lower bulk modulus; the resonant hybridization part explains about 20% of the observed B for Zn and 15% for Cd. In order to know the effect of neglecting the hybridization potential in the lattice dynamics, we have calculated the phonon frequencies of Zn with $A_d=0$. This neglect results in lowering the phonon spectrum of Zn in general in the range 25–30%. For comparison we present the results of this calculation at

some zone boundary points with those of the full RMP in Table IV. This shows that an accurate description of the nonlocal d -wave scattering is required to get a correct phonon spectrum. This requirement is met by the RMP which, describing the nonlocal ionic d potential in terms of the hybridization coefficient $\gamma(k)$, provides an accurate description of the $l=2$ phase shift over the whole valence band.⁸

On the other hand, the generalized pseudopotential theory (GPT) leads to a different conclusion: The hybridization part has very little effect on the zinc phonon spectrum.²¹ We are not able to give a definite explanation of this discrepancy but we believe it to be related to the following points: (i) The zinc and cadmium structural energies and phonon spectrum are determined mainly by the near-Fermi-level part of the structure-dependent equivalent pseudo- or model-Hamiltonian, as shown below. (ii) Although the near resonant ($E \approx E_d \ll E_F$) hybridization is a well-defined quantity (directly related to the physical hybridization gap³), its continuation far away from the resonance is expected to be strongly model dependent.

TABLE IV. Phonon frequencies for Zn at some zone boundary points (in 10^{12} Hz).

Phonon frequency	RMP with A_d	RMP with $A_d=0$	AMP	Experiment (Ref. 28)
$\Delta_2(A)$	3.30	2.44	3.10	2.92
$\Delta_6(A)$	1.89	1.21	1.80	1.86
$\Sigma_1^U(M)$	6.96	5.59	6.84	6.44
$\Sigma_1^L(M)$	6.82	5.48	6.76	6.11
$\Sigma_3^U(M)$	3.19	2.25	3.07	2.70
$\Sigma_3^L(M)$	1.63	1.37	1.65	2.02
$\Sigma_4^U(M)$	4.31	3.28	4.31	3.72
$\Sigma_4^L(M)$	3.80	2.97	3.77	3.52

We discuss first very briefly the GPT. Its object is to go beyond the small core approximation of the simple-metal pseudopotential theory (PT). The neglect of the hybridization and overlap contributions amounts precisely to use a small core approximation even for the d states. The phonon results²¹ show that this approximation is quite good for zinc. Agreement with the following discussion for the RMP is obtained if one assumes that the PT Hamiltonian is a good one near the Fermi level, far away from the resonance.

The strong near resonance hybridization effect in the RMP can be studied as follows. We consider a simple-metal-like model potential derived from the RMP by replacing $v_{\text{res}}(E)$ by the "associated" model potential (AMP):

$$v_A(E) = v_{\text{res}}(E_F) + (E - E_F) \frac{\partial}{\partial E_F} v_{\text{res}}(E_F),$$

which is nonresonant but approximates the resonant part near the Fermi level [there is little point in going beyond the linear approximation since we do not want to go beyond the second approximation in $(E_F - E_d)^{-1}$]. The AMP $w + v_A$ is nearly equivalent to $w + v_{\text{res}}$ for $E \approx E_F$ and is quite different in the strong hybridization region

$E \approx E_d$. The comparison between an AMP result and the corresponding RMP result gives then the effect of the strong near-resonance hybridization.

In order to do this comparison, we have recalculated the structural energies, bulk modulus, and phonon frequencies for the AMP. Very small differences with the RPM (Table III) results are obtained. The bulk modulus is a few percent smaller. For example, the AMP result for Zn is 0.579 to be compared to 0.591 for the RPM (in units of 10^{21} cgs). Phonon frequencies of Zn in general are lowered by 5% approximately (Table IV). The conclusion thus is that the strong near-resonance hybridization has a small effect. On the other hand, the concept of hybridization is not well defined far away from the resonance; even in the framework of the RMP theory $v_{\text{res}}(E)$ is only a part of the total ionic d potential and its value, when $E \approx E_F \gg E_d$, is model dependent: The choice of the d nonresonance part in (2) is quite flexible and different choices would lead to different v_{res} since the equivalence requirement determines only the total ionic d potential. v_{res} is found to have a very significant effect when the present work choice (1) is done, but we cannot assert that this is intrinsically a hybridization effect.

-
- ¹J. M. Ziman, Proc. Phys. Soc. London **86**, 337 (1965).
²J. Hubbard, Proc. Phys. Soc. London **92**, 921 (1967).
³V. Heine, Phys. Rev. **153**, 673 (1967).
⁴R. A. Deegan, Phys. Rev. **188**, 1170 (1969).
⁵L. Dagens, J. Phys. C **8**, L581 (1975).
⁶L. Dagens, J. Phys. F **6**, 1801 (1976).
⁷L. Dagens, J. Phys. F **7**, 1167 (1977).
⁸L. Dagens, Phys. Status Solidi B **84**, 311 (1977).
⁹J. C. Upadhyaya and L. Dagens, J. Phys. F **8**, L21 (1978).
¹⁰J. C. Upadhyaya and L. Dagens, J. Phys. F **9**, 2177 (1979).
¹¹E. G. Brovman, Yu Kagan, and A. Kholas, Fiz. Tverd. Tela. (Leningrad) **11**, 896 (1969) [Sov. Phys.—Solid State **11**, 733 (1969)].
¹²G. Gilat, G. Rizzi, and G. Cubotti, Phys. Rev. **185**, 971 (1969).
¹³O. P. Kulshrestha and J. C. Upadhyaya, Pramana **6**, 291 (1976).
¹⁴J. Kumar and J. C. Upadhyaya, Phys. Rev. B **19**, 866 (1979).
¹⁵H. Eschrig and H. Wonn, Phys. Status Solidi **40**, 163 (1970).
¹⁶J. A. Moriarty, Phys. Rev. B **1**, 1363 (1970); **6**, 1239 (1972).
¹⁷W. A. Harrison, Phys. Rev. **181**, 1036 (1969).
¹⁸J. A. Moriarty, Phys. Rev. B **10**, 3075 (1974).
¹⁹J. A. Moriarty, Phys. Rev. B **16**, 2537 (1977).
²⁰W. Kohn and L. J. Sham, Phys. Rev. **140**, A1133 (1965).
²¹J. Panitz, P. H. Cutler, and W. F. King III, J. Phys. F **4**, L106 (1974).
²²P. H. Cutler, R. Day, and W. F. King III, J. Phys. F **5**, 1801 (1975).
²³W. A. Harrison, *Pseudopotentials in the Theory of Metals* (Benjamin, New York, 1966).
²⁴R. W. Shaw, J. Phys. C **2**, 2335 (1969).
²⁵P. W. Anderson, Phys. Rev. **124**, 41 (1961).
²⁶J. A. Reissland and O. Ese, J. Phys. F **5**, 110 (1975).
²⁷J. C. Upadhyaya and A. O. E. Animalu, Phys. Rev. B **15**, 1867 (1977).
²⁸L. Almqvist and R. Stedman, J. Phys. F **1**, 785 (1971).
²⁹G. Toussaint and G. Champier, Phys. Status Solidi B **54**, 165 (1972).
³⁰D. C. Wallace, Phys. Rev. **182**, 778 (1969).
³¹K. A. Gschneidner, in *Solid State Physics*, edited by F. Seitz and D. Turnbull (Academic, New York, 1964), Vol. 16, p. 276.